19 INTERNATIONAL CONGRESS ON ACOUSTICS
MADRID, 2-7 SEPTEMBER 2007

MODELING AND MEASUREMENT OF WIND INSTRUMENT BORES

PACS: 443.75.Zz

Smyth, Tamara[1]; Abel, Jonathan[2]
[1]School of Computing Science; Simon Fraser University; British Columbia, Canada; tamaras@cs.sfu.ca
[2]Center for Computer Research in Music and Acoustics; Stanford University; Stanford, California 94305-8180 USA; abel@batnet.net

ABSTRACT
One dimensional digital waveguides are widely used to model travelling pressure waves along wind instrument bores. These models must also account for frequency-dependent losses occurring along the bore walls, and at boundaries. This is accomplished by incorporating waveguide filter elements, which are based on the widely accepted theory describing these losses. A measurement technique is demonstrated that allows the effects of each waveguide element to be isolated and observed for simple cylindrical and conical tube structures, as well as their combination. This measurement system yields data that closely matches the theory and provides confidence that it may be extended to accurately measure musical instrument bores, where bore shapes are usually considerably less simple, and thus more difficult to account for theoretically. This work paves the way for further application to clarinet and trumpet bores.

INTRODUCTION
We have developed a measurement system for simple acoustic tube structures, a continuation of the work presented at [1], that allows observation of waveguide model components. The measurements closely correspond to digital waveguide theory, allowing validation of the system before using it on more complex tube structures such as the bores of musical instruments.

DIGITAL WAVEGUIDE THEORY
It is well known that the right and left travelling pressure waves in both cylindrical and conical tubes can be modeled using a digital waveguide, or bi-directional delay line. In practice, is is also

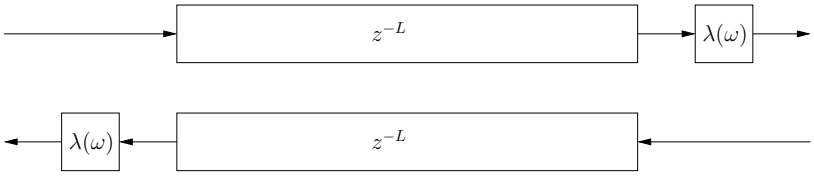

Figure 1: A waveguide section.

necessary to account for any losses that occur during propagation. The effects of viscous drag and thermal conduction along the bore walls, lead to an attenuation in the propagating waves [2] approximated by

$$\alpha(\omega) \approx 2 \times 10^{-5} \sqrt{\omega}/a, \tag{1}$$

leading to a round trip attenuation for a tube of length L given by

$$\lambda^2(\omega) = e^{-2\alpha(\omega)L}. \tag{2}$$

In conical structures diverging to the right, there's an additional loss of $1/r$ in the right travelling wave due to spherical spreading, where r is the distance from the observation point to the cone apex. For left travelling waves, however, there is a reconcentration of the the pressure wave proportional to r.

Any change of wave impedance in the waves, which may take the form of a termination or connection to another waveguide section, will require additional filtering to account for reflection and possibly transmission.

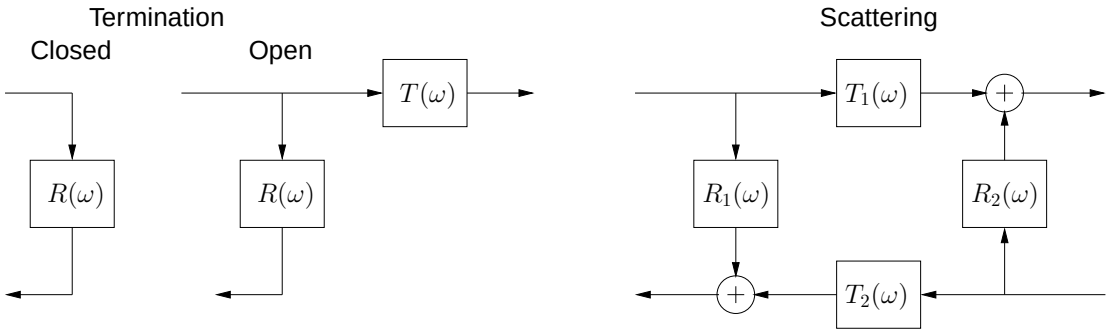

Figure 2: A change of impedance in a waveguide section may occur as a termination (closed with perfect reflection and open with reflection with corresponding transmission) or scattering junction when connected to another section.

A change in cross sectional area of a tube will change the wave impedance, resulting in a reflection with frequency-dependent losses following the expression

$$R(\omega) = \frac{Z_2/Z_1 - 1}{Z_2/Z_1^* + 1}, \tag{3}$$

where Z_2 and Z_1 are the new and previous wave impedances, respectively, which for plane pressure waves in cylindrical tubes, and spherical pressure waves in conical tubes, are given by

$$Z_y = \frac{\rho c}{S}, \quad \text{and} \quad Z_n = \frac{\rho c}{S}\frac{j\omega}{j\omega + c/x}, \tag{4}$$

respectively [3]. A special case of a change in cross section is when the wave reaches an open end, and subsequently, open air. In this case, the complex terminating impedance $Z_2(\omega) = Z_L(\omega)$, is a fairly complicated function of frequency, which is given by Levine and Schwinger in terms of Bessel and Sturve functions functions [4]. Here we approximate the reflection and transmission functions using first order low-pass and hi-pass filters. An example waveguide model of a cylinder

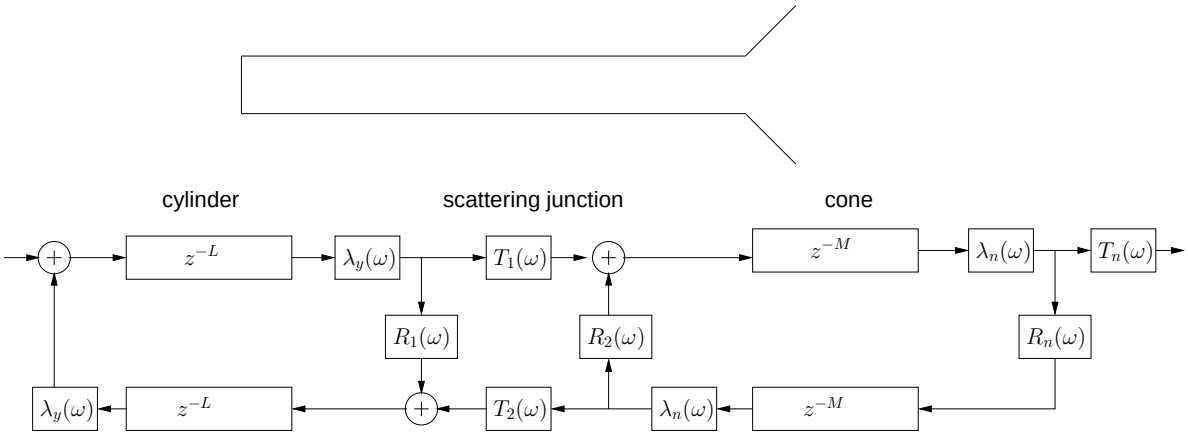

Figure 3: Example waveguide models of the open cylicone.

with a connected cone incorporates all of these waveguide elements, including transmission filters $T(\omega)$, which are the complement of the reflection filters $R(\omega)$, as seen in Figure 3.

MEASUREMENT TECHNIQUE

It's well known that inputting an impulse into an LTI system, yields the impulse response of the system. There are problems, however, in using an impulse as the test signal to obtain an accurate measurement of the response. Since there must be sufficient energy in the test signal to excite the system above the noise floor, the amplitude of the impulse would have to be quite high, and would likely result in distortion. We therefore use a sinusoid that is swept over a frequency trajectory, in this case exponential, effectively smearing the energy in a loud impulse over a period of time. Doing so, drives the system with a large amount of energy without distortion.

To isolate each of the waveguide model elements seen in Figure 3, the test signal was input through a speaker at one end of each of four specially developed tube structures (see Figure 4). A microphone at the same end as the speaker recorded the response.

1. **Cylinder, closed end.** A 2 meter long cylinder is closed at one end to ensure a perfect reflection, allowing transfer functions to be estimated for the speaker output $\sigma(\omega)$, the speaker reflection $\rho(\omega)$, and the wall loss filters $\lambda(\omega)$. The arrival responses L_n for this measurement may be seen in Figure 7.

2. **Cylinder, open end.** Opening the cylinder allows us to estimate the transfer function of the reflection at the open end of a cylinder, $R_{op}(\omega)$, and compare the result with the theory given by Levine and Schwinger.

3. **Cylicone, closed end.** The addition of a conical flare with a spherical termination (to ensure a perfect reflection) to the above cylindrical tube allows the effects of reflection and transmission at the junction to be observed .

4. **Cylicone, open end.** Opening the conical end allows us to observe the effects of the reflection at the end of an open cone.

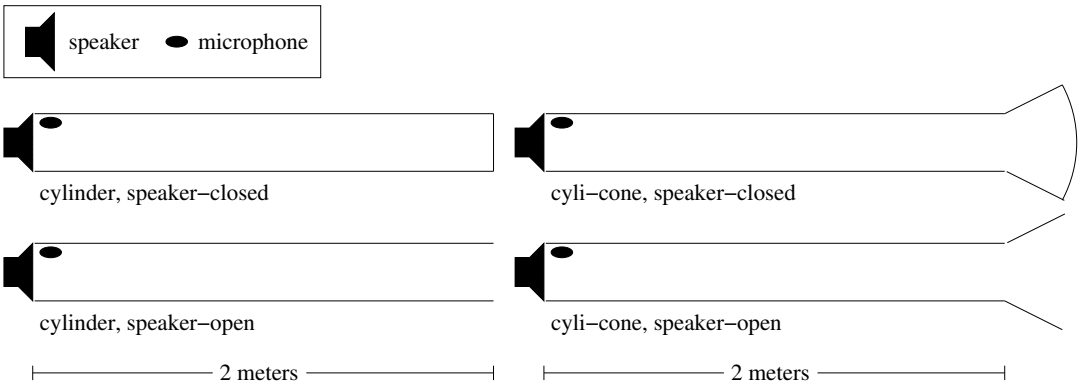

Figure 4: Four simple tube structures: cylinder (closed and open) and cylicone (closed and open).

MEASURED RESPONSES

Given the arrival responses for a closed cylinder, L_n, we are able to estimate the transfer function of the reflection off the speaker (which has a prominent hi-pass characteristic as they are designed to be resonant at low frequencies). We begin by considering the first arrival, which is the output of the speaker measured at the mic, and consists solely of the speaker transfer function:

$$L_1 = \sigma(\omega). \tag{5}$$

The following arrival, L_2, consists of the sum of left and right traveling pressure waves at the microphone position: the speaker transfer function after having travelled, round-trip, the length of the tube, given by $\sigma(\omega)\lambda^2(\omega)$, and the speaker transfer function with round trip losses after reflecting off the speaker, $\sigma(\omega)\lambda^2(\omega)\rho(\omega)$. The second arrival may therefore be expressed as their sum, and is given by

$$L_2 = \sigma(\omega)\lambda^2(\omega)(1 + \rho(\omega)). \tag{6}$$

Each subsequent arrival for the closed cylinder consists of the previous arrival, with round-trip wall losses of $\lambda^2(\omega)$. The third arrival is therefore given by

$$L_3 = \sigma(\omega)\lambda^4(\omega)(1+\rho(\omega)). \tag{7}$$

These three responses are sufficient for estimating the speaker reflection transfer function. The speaker reflection $\rho(\omega)$ is isolated and an intermediate variable is defined:

$$\zeta(\omega) = \frac{L_1 L_3}{(L_2)^2} = \frac{\rho(\omega)}{1+\rho(\omega)}, \tag{8}$$

yielding an estimate for the speaker transfer function given by

$$\hat{\rho}(\omega) = \frac{\zeta(\omega)}{1-\zeta(\omega)}. \tag{9}$$

With the estimate of the speaker transfer function, we may also use two of the arrival responses to estimate the round-trip wall loss transfer function, given by

$$\hat{\lambda}^2(\omega) = \frac{L_3}{\hat{\rho}(\omega)L_2}. \tag{10}$$

Opening up the end of tube allows us to obtain arrival responses Y_n, shown in Figure 7 b, from which the open-end reflection transfer function R_{op} may be isolated. As with the closed cylinder, the initial response of this measurement is merely the response of the speaker to an impulse, yielding the speaker transfer function, $Y_1 = \sigma(\omega)$. The second arrival, Y_2, is similar to L_2 but also includes the effects of the open-end reflection, and is given by

$$Y_2 = \sigma(\omega)\lambda^2(\omega)R_{op}(\omega)(1+\rho(\omega)). \tag{11}$$

Subsequent arrival responses include the effects of additional round-trip wall losses and open-end reflections.

Given the second arrival for the closed tube, L_2, and the second arrival for the open tube, we are able to estimate the reflection from an open end through a deconvolution:

$$\hat{R}_{op}(\omega) = \frac{Y_2}{L_2}. \tag{12}$$

In results not presented here, estimated wall losses and the open tube reflection function, were seen to match that theoretically predicted to within a fraction of a dB across the audio band.

Attaching a conical flare to the cylindrical tube, and terminating with a spherical cap to ensure a perfect reflection, allows us to observe the effects of the reflection and transmission filters the junction. In this case, we must look at the individual *subarrivals* within the second arrival A_2 of Figure 7. The first *subarrival* $A_{(2,1)}$ has a response similar to Y_2, except it includes a reflection off the junction R_y (as seen from the cylinder), instead of at the open-end. Anything that is not reflected at the junction is transmitted through to the conical section with losses described by the transfer function T_y, and is subject to round-trip conical wall losses given by $\lambda_n^2(\omega)$, before being transmitted back through the junction to the cylinder with losses described by $T_n(\omega)$. The second subarrival may therefore be described by the expression

$$A_{(2,2)} = \sigma(\omega)\lambda_y^2(\omega)\lambda_n^2(\omega)T_y(\omega)T_n(\omega)(1+\rho(\omega)). \tag{13}$$

Though it is difficult to actually estimate filters corresponding to R_y and R_n using the measurement data, as there is insufficient decay between *subarrivals* to obtain clean estimates, we may model each subarrival following the theory used to obtain 13, observe each *subarrival* independently, and then see how the combined result compares to the whole of the measured closed-cone arrival A_2. The arrival responses for the open cylicone, from which we may observe the effects of a conical open-end reflection R_n, are treated in the same way as for the closed (though their *subarrivals* are even more blurred and difficult to observe). The results for both are seen in Figures 5 and 6, each showing a very close match between model and measurement.

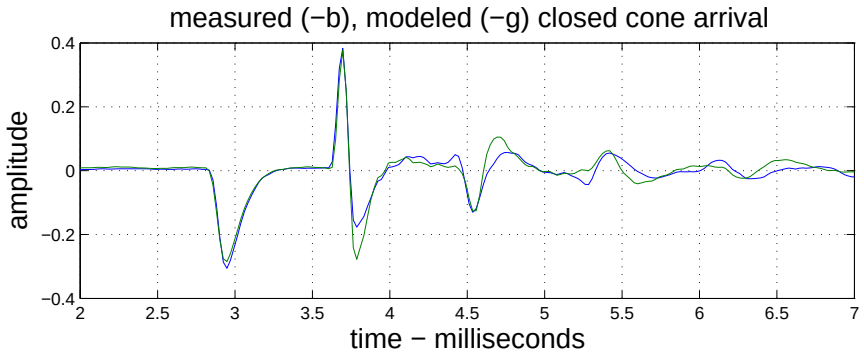

Figure 5: Measured and modeled closed cone second arrival (corresponding to $A_{(2,2)}$).

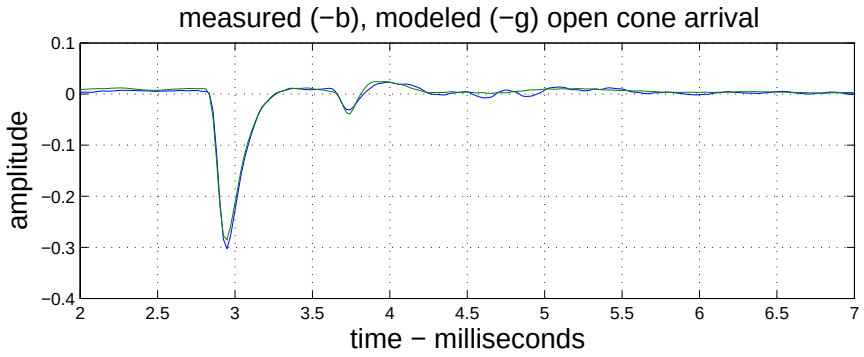

Figure 6: Measured and modeled open cone second arrival (corresponding to $N_{(2,2)}$).

CONCLUSIONS

An approach for measuring waveguide model element transfer functions is presented using a speaker to drive an acoustic tube, with a co-located microphone recording the response. The tube responses, each with a different termination, were used to estimate wall losses, and various reflection and transmission filters with excellent agreement to theoretical prediction. As a result, it is thought that the reflection function of a wind instrument can be accurately estimated by comparing the response of a rigidly-terminated tube to one that is terminated with an instrument.

ACKNOWLEDGMENT

We would like to sincerely thank John Lundell, Carr Wilkerson, and Harrison Smith for their help in fabricating the experimental setup, Theresa Leonard, and the Banff Centre for the Arts, for the use of their facilities, and the Natural Sciences and Engineering Research Council of Canada (NSERC) for their support.

References:

[1] Tamara Smyth and Jonathan Abel, "Observing the effects of waveguide model elements in acoustic tube measurements," in *152nd Meeting of the Acoustical Society of America (ASA)*, Honolulu, Hawaii, November 2006, vol. 120, p. 3331.

[2] Jonathan Abel, Tamara Smyth, and Julius O. Smith, "A simple, accurate wall loss filter for acoustic tubes," in *DAFX 2003 Proceedings*, London, UK, September 2003, International Conference on Digital Audio Effects, pp. 53–57.

[3] David P. Berners, *Acoustics and Signal Processing Techniques for Physical Modeling of Brass Instruments*, Ph.D. thesis, Stanford University, Stanford, California, July 1999.

[4] Harold Levine and Julian Schwinger, "On the radiation of sound from an unflanged circular pipe," *Phys. Rev*, vol. 73, no. 4, pp. 383–406, 1948.

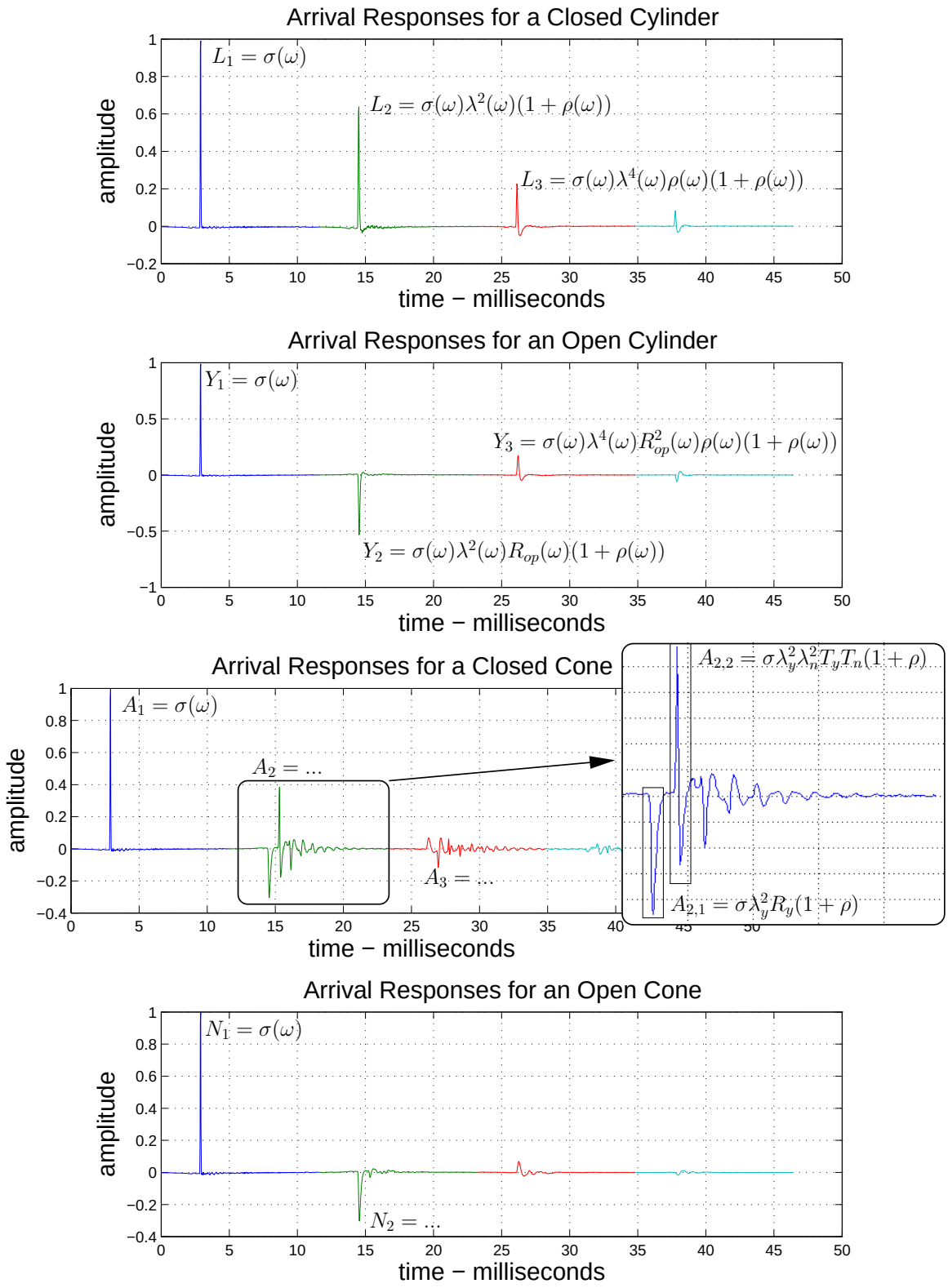

Figure 7: Arrival responses are shown with their corresponding transfer functions. The transfer function in $A_{2,1}$ and $A_{2,2}$ are functions of frequency, with ω omitted in the interest of saving space. The response $A_{2,1}$ shows a low-pass characteristic expected of a junction reflection, while $A_{2,1}$ shows a hi-pass characteristic expected of two transmissions through the junction.